applied sciences

MDPI

Article

Research on Mechanical Properties and Failure Mode of Conglomerate Based on Discrete Element Method

Jiawei Zhang, Xiangjun Liu *, Jian Xiong, Lixi Liang and Wen Zhang

State Key Laboratory of Oil and Gas Reservoir Geology and Exploitation, Southwest Petroleum University, Chengdu 610500, China
* Correspondence: liuxj@swpu.edu.cn

Abstract: Conglomerate reservoir is an important part of unconventional oil and gas resources, which has great developmental potential. However, its sedimentary environment and structural background are complex, and its cementation types, gravel volume fraction and shape are quite different, which leads to its strong heterogeneity. When developing a conglomerate reservoir, it is extremely difficult to drill because of its strong heterogeneity. It is difficult to obtain the mechanical properties and laws of the conglomerate through physical experiments, which further restricts the development process of conglomerate reservoirs. In order to study its failure law, a three-dimensional numerical model of a conglomerate is built based on the discrete element method, and the effects of cementation strength and gravel characteristics on the mechanical properties of the conglomerate are emphatically studied. The results show that the elastic modulus and uniaxial compressive strength of the conglomerate decrease obviously with the decrease in cementation strength. With the increase in cementation strength, the normal contact force of the conglomerate model increases significantly, the distribution of normal contact force changes from cylinder to sphere, and the heterogeneity of the conglomerate decreases. There is a threshold value for the influence of cementation strength on mechanical properties of the conglomerate, and when the threshold is exceeded, the mechanical properties of the conglomerate no longer change obviously. With the increase in gravel content, the uniaxial compressive strength of the conglomerate decreases at first and then increases, the phenomenon of penetrating gravels and bypassing gravels increases, and the single diagonal crack changes into diagonal cross cracks; the cementation strength and gravel content of gravel jointly affect the mechanical properties and fracture morphology of the conglomerate, and its stress–strain relationship is the external macroscopic expression of normal contact force of internal particles.

Keywords: conglomerate; cementitious strength; mechanical properties; crack propagation; discrete element; three-dimensional

check for updates

Citation: Zhang, J.; Liu, X.; Xiong, J.; Liang, L.; Zhang, W. Research on Mechanical Properties and Failure Mode of Conglomerate Based on Discrete Element Method. *Appl. Sci.* **2023**, *13*, 223. https://doi.org/10.3390/app13010223

Academic Editor: Francesco Tornabene

Received: 4 December 2022
Revised: 18 December 2022
Accepted: 20 December 2022
Published: 24 December 2022

1. Introduction

With the march of China's oil industry and the progress of exploration and development technology, the development of unconventional oil and gas resources has become the focus of global oil and gas research, and has become the next key research object of oil and gas exploration and reservoir development in China [1]. Unconventional oil and gas resources include tight sandstone gas, shale gas, tight oil, coalbed methane, etc. Tight oil and gas resources feature a short investment cycle, and tight oil and gas are stored in sandstone or conglomerate reservoirs. In 2018, the world's largest glutenite oilfield was discovered in Xinjiang, with confirmed reserves of about 520 million tons. [2] The conglomerate reservoir generally is characterized by low porosity and low permeability, which results in an insufficient self-production capacity. Therefore, it is necessary to master its mechanical properties and improve reservoir permeability by hydraulic fracturing.

Conglomerate reservoirs in China are mainly distributed in northwestern Junggar Basin, Karamay Oilfield, Bohai Bay Basin, Fute Oilfield of Erlian Basin and Dongxin Area of Shengli Oilfield [3,4]. Conglomerate reservoirs are mainly developed in fault zones with complex sedimentary environments and tectonic settings, which determine their strong heterogeneity and complex mechanical properties. Researchers at home and abroad have studied the influence of gravel on the mechanical properties of a conglomerate through physical experiments and numerical models and proved the strong heterogeneity of the conglomerate. The existence of gravel has a great impact on the mechanical strength of the cementation surface, and the cementation mode can be divided into argillaceous, calcareous cementation or semi cementation [5]. Chen [6] and Ju [7] studied conglomerates with different cementation strengths in Mahu, Xinjiang, and found that cementation strength has a significant influence on mechanical properties and fracture propagation of conglomerates. Liu [8] and Khanlari [9] found that the conglomerate shows strong heterogeneity and stress concentration due to the existence of gravel, which leads to the linear decrease in compressive and tensile strength of the conglomerate with the increase in gravel content. In order to study the influence of gravel content on conglomerates, researchers used natural and artificial cast rock samples to study the influence of gravel sorting and different particle sizes on the mechanical properties and deformation parameters of conglomerates [10–13]. Physical experiments are interfered by external factors and have limitations such as non-repeatability, so numerical simulation and other means have been widely used. Through RFPA, ABAQUS and other finite element software, it is found that cracks in gravel mainly show four propagation modes [14–16]. The finite element method has some limitations, such as the mesh cannot update the data in real time and it is difficult to divide the mesh at the crack tip. However, there are great similarities in cementing modes between particles and 'gravel and matrix' in the discrete element method, which is more suitable for analyzing discontinuous media materials such as a conglomerate. Therefore, researchers began to use the discrete element method to analyze discontinuous media materials such as the conglomerate [17]. Luo [18] used the discrete element method to divide the conglomerate into a composite medium composed of three parts: gravel, matrix and cementation surface. The critical energy release rate was used to study the mechanical properties and fracture propagation law of gravel with different particle sizes, contents and fracture toughness. Han [19] and Lei [20] used PFC^{2D} to construct broken particle clusters with different particle sizes to study the mechanical properties evolution and heterogeneity effect of the conglomerate under uniaxial compression. The above research has important guiding significance for exploring the mechanical properties of the conglomerate and the law of crack extension, but the relationship between the mechanical properties of the conglomerate and gravel characteristics, contact mode and cementation strength has not been studied. In addition, when the two-dimensional discrete element model is used to simulate the three-dimensional material, the components of several forces of the particles are not fully considered, the correlation between porosity and actual calculation is poor, and the calculation of strain and stress is greatly constrained.

In this paper, a three-dimensional numerical model of a conglomerate is established by the discrete element method to study the influence of gravel characteristics and cementation strength on mechanical properties and fracture propagation of the conglomerate. The mechanical parameters such as stress, strain and elastic modulus were extracted to analyze the mechanical properties and crack propagation law of the conglomerate. On this basis, the influence of cementation strength and gravel characteristics on the heterogeneity and macroscopic mechanical properties of the conglomerate is explored by combining the micromechanical parameters and distribution characteristics of conglomerate model particles. The research results provide a relevance for the formulation of a hydraulic fracturing construction scheme for conglomerate reservoirs.

2. Gravel Model Based on Discrete Element Method

2.1. Discrete Element Method

The discrete element method can well simulate the evolution of rock mechanical properties, crack nucleation, propagation and extension, and is widely applied in the field of rock mechanics [21,22]. In the discrete element method, particles are used to represent rock materials, bonds are used to represent bonding between particles, and parallel bonding is used in the bonding model. Parallel bonding is similar to a spring with shear stiffness and normal stiffness between particles, which can transmit force and moment. When bonding is formed, the relative movement of particles at the contact point forms force and moment. When the force and moment on the contact surface exceed its maximum bonding strength, the parallel bonding will break and the force and moment between particles will be removed. The constitutive model is shown in Figure 1 and Formula (1). In Figure 1 Bond model, g_s is reference gap, $\overline{k}_s$ is tensile strength, k_s shear stiffn, k_n normal stiffness, $\overline{k}_n$ is parallel bond normal stiffness $\overline{k}_s$ is parallel bond shear stiffn $\overline{c}$ is cohesion $\overline{\Phi}$ is friction angle. The failure criterion is close to the real failure of rock, so the parallel bond model is used for a follow-up study in this paper.

$$\overline{\sigma} = \frac{\overline{F}_N}{\overline{A}} + \overline{\beta}\frac{\|\overline{M}_b\|\overline{R}}{\overline{I}} \tag{1}$$

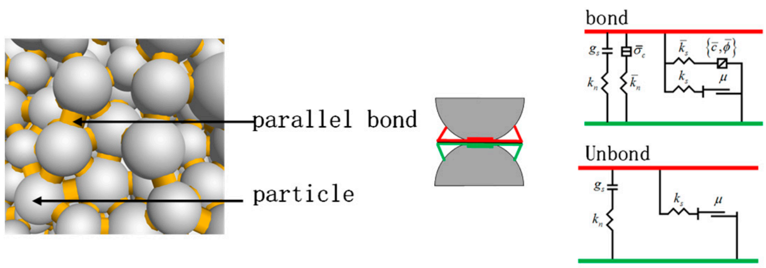

Figure 1. Parallel bonding model.

In Formula (1), $\overline{F}_N$ is the normal force at the contact point; $\overline{M}_b$ is the bending moment and torque of the contact point; $\overline{R}$ is the average radius of the two contact particles; $\overline{A}$ is the cross-sectional area of the sphere; $\overline{I}$ is the moment of inertia; $\overline{\beta}$ is the moment contribution coefficient.

2.2. Establishment of the Conglomerate Model and Parameter Calibration

Taking the conglomerate as the research object, the discrete element numerical model is established to study the mechanical properties and failure morphology of the conglomerate. The conglomerate sample is taken from the depth of 3109~3259 m in Mahu Sag of Baikouquan Formation, Xinjiang. The gravel content is between 30~70%, the particle size is 5~70 mm, and the mineral composition is mainly compacted and cemented by quartz, feldspar and clay. Since gravel is a destructive material, this model uses particle clusters with strong strength to simulate gravel with high hardness. The model consists of matrix, cementation surface and gravel, as shown in Figure 2.

The discrete element model reflects the adhesion between particles. Therefore, the meso-parameters assigned to the model need to reflect the mechanical properties of adhesion between particles, which cannot be obtained directly in laboratory tests. When assigning parameters, researchers usually take the stress–strain curve and failure mode of rock obtained by indoor experiments as relevance, and use the "trial-and-error method" to adjust the meso-parameters of the model. The results of the model are basically consistent with the stress–strain curve and failure mode of indoor tests [23,24], and the meso-parameters obtained by trial-and-error are usually considered to be correct. Namely, the numerical model can reflect the mechanical properties and failure modes of indoor experimental samples. TCR-100 high temperature and high-pressure rock triaxial rheometer is used as the loading system for indoor uniaxial test, and the maximum axial load of the tester is 2000 kN.

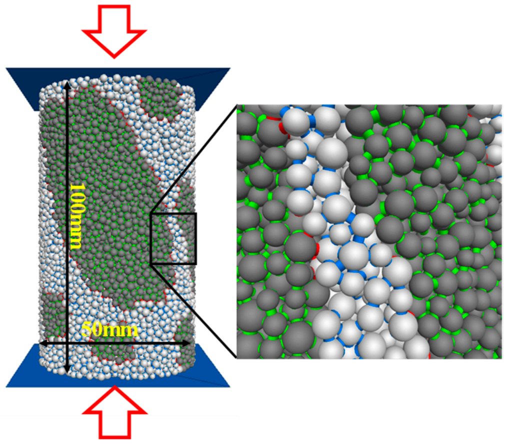

Figure 2. Numerical model of the conglomerate (green represents gravel bond; blue represents matrix bond; red represents cementation surface of gravel and matrix).

The experiment works in displacement-control loading mode, and the loading rate is 1 mm/min. The stress–strain curve and the failure mode of the conglomerate are used as the comparison of the assignment of the meso-parameters. As shown in Figure 2, the standard size of model is Φ 50 × 100 mm, 34,142 particles in total, 91,239 parallel bonds in the model, and the loading speed is consistent with the indoor experiment. Meso-parameters are adjusted through continuous trial-and-error, and the relationship between meso-parameters and macro-parameters are analyzed according to Zhang [25]. Firstly, the Parallel bond tensile strength and Parallel bond cohesion in the meso-parameters of gravel, matrix and cementation region are adjusted to make the peak strength of the conglomerate numerical model consistent with the peak strength of the physical experiment. Secondly, the Parallel bond module is adjusted to make the elastic modulus of the conglomerate numerical model consistent with the elastic modulus of the physical experiment, and finally the Friction coefficient is adjusted to make the fracture propagation pattern of the conglomerate numerical model similar to that of the physical experiment. The mesoscopic parameters adjusted by the trial-and-error method are shown in Table 1. The meso-parameters of the numerical model are shown in Table 1, and the results of indoor experiments and numerical models are shown in Figure 3. The results show that the data of the indoor experiment are basically consistent with the data of the numerical model, and bypassing gravels mainly occurs in crack propagation; the errors of peak strength and elastic modulus are 2.08% and 3.11%, respectively, indicating that the meso-parameters are feasible.

Table 1. Meso-parameters.

Meso-Parameters	Gravel	Matrix	Cementation between Gravel and Matrix
Particle density/Kg m^3	2700	2700	/
Particle radius ratio	1.66	1.66	1.66
Porosity/%	5	5	/
Friction coefficient	0.8	0.577	0.377
Parallel bond module/GPa	25.5	10.5	85
Ratio of parallel bond strength	1.8	1.2	1.0
Parallel bond internal friction angle/°	38.5	33.5	30.5
Parallel bond tensile strength/MPa	60	30	15
Parallel bond cohesion/MPa	70	45	20

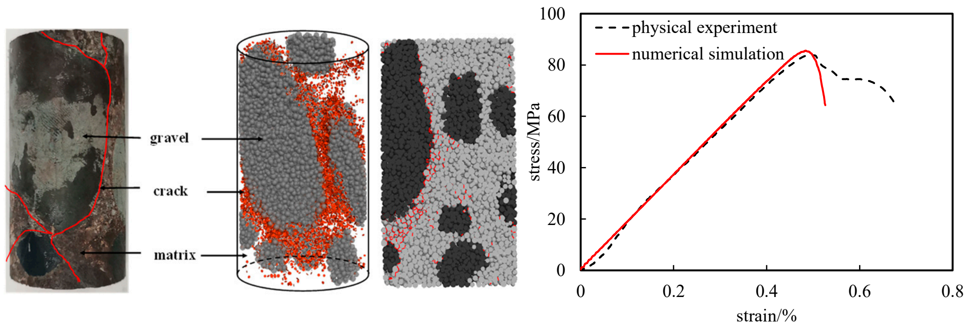

(a) (b)

Figure 3. Physical test and numerical model results. (**a**) Failure mode; (**b**) stress–strain curve.

3. Research Process

The sedimentary environment, size, content and composition of gravel are quite different in Mahu sag, which will affect the mechanical properties and failure patterns of the conglomerate. The research mainly studies the effects of cementation strength between gravel and matrix, gravel content and morphology on mechanical properties and fracture propagation of the conglomerate.

3.1. Response of Cementation Strength between Gravel and Matrix

Common cementation types in conglomerates are argillaceous cementation and calcareous cementation, and different cementation types lead to different cementation strength. When the conglomerate is subjected to external force, the strength of the cementation surface between gravel and matrix has obvious influence on the mechanical properties and fracture propagation of the conglomerate. In order to reduce the influence of gravel particle size on numerical simulation results, the numerical model selects particles with an approximately equal size to simulate, and studies the influence of cementation strength on mechanical properties and fracture propagation of the conglomerate by adjusting different mechanical parameters of the cementation surface between gravel and matrix. The deformation parameters, strength parameters and friction coefficient in the numerical model are set to 0.1~1.0 times that of gravel, while the other parameters remain unchanged. A uniaxial compression test was carried out to study the influence of different cementation strength on macroscopic mechanical properties of the conglomerate. Set the parameters in advance and specify the loading speed as 1 mm/min to ensure that the loading is quasi-static.

The simulation results are shown in Figure 4. The uniaxial compressive strength and elastic modulus of conglomerate decrease significantly when the ratio of gravel–matrix strength to gravel strength decreases from 0.4 to 0.1. When the bond strength ratio is reduced from 1 to 0.4, the uniaxial compressive strength and elastic modulus bring no apparent change. It can be seen from the cumulative number of fractures that the lower the cementation strength ratio, the lower the corresponding pressure when fractures begin to occur in the rock. Due to the gravel, matrix and cementation area of the conglomerate bear axial loading pressure at the same time. When the cementation strength is low, the strength of the cementation area is obviously lower than that of the gravel and matrix area. With the increasing axial pressure, the cementation area will be destroyed, and cracks will occur when the axial pressure reaches the ultimate bearing capacity of the cementation area. Therefore, with the decrease in cementation strength ratio, the fracturing of rock will be lower when cracks begin to appear. As shown in Figure 4, when the cementation strength ratio is less than 0.4, the number of fractures witnesses a surge at the initial stage of loading. Combined with the fracture distribution map during conglomerate failure (Figure 5), it can be seen that the fractures generated at the initial stage of loading are caused by shear force of the cementation surface between gravel and matrix. When the cementation strength ratio is more than 0.4, the number of fractures in the conglomerate tends to be stable at the initial stage of loading, and most of the fractures occur at the peak strength of loading.

By comparing the influence of cementation strength ratio on mechanical properties of the conglomerate, the relationship between cementation strength ratio and uniaxial compressive strength, elastic modulus, cumulative fracture number and fracture initiation pressure is statistically analyzed. As shown in Figure 6, the uniaxial compressive strength, elastic modulus, cumulative number of cracks and crack initiation pressure vary with the cementation strength ratio. Fracture initiation pressure and the axial stress point of the first fracture in the corresponding rock sample are essential parameters to evaluate the occurrence of cracks in rock. When the cementation strength ratio is less than 0.4, the uniaxial compressive strength increases rapidly as shown in Figure 6a. The cumulative number of cracks corresponds to the total number of cracks produced in rock after compression. When the cementation strength ratio is 0.4, the variation laws of cumulative number of cracks, elastic modulus and crack initiation strength all reach critical values as shown in Figure 6b–d. When the cementation strength is greater than 0.4, the crack initiation pressure, elastic modulus and cumulative number of cracks tend to be stable. This can be seen from the cumulative crack–strain curve. When the cementing strength is greater than 0.4, there is no distinct change in the number of cracks before the peak strength. By analyzing the curves of four mechanical parameters and the cumulative number of cracks, it can be seen that when the cementing strength ratio is 0.4, it is the critical value of the change of mechanical parameters. At this time, the mechanical properties of the conglomerate are gradually determined by the matrix, and the cementation strength ratio is no longer the dominant factor affecting the mechanical properties of the conglomerate.

In order to visualize the propagation of fractures in rock, the three-dimensional discrete element model is sliced and projected onto a two-dimensional plane as shown in Figure 5a. It can be seen that when the cementation strength ratio is less than 0.4, a large number of annular shear fractures and tensile fractures passing through the matrix form a complex fracture network around the gravel after the failure of rock samples. When the cementation strength ratio is greater than 0.4, the cumulative number of cracks tends to be stable, the shear failure of cementation surface decreases, and the failure mainly occurs between gravel, forming tensile failure accompanied by gravel penetration, as shown in Figure 5b. To sum up, the cementation strength between gravel and matrix in the conglomerate has obvious influence on the mechanical properties and fracture propagation of the conglomerate. Therefore, the conglomerate with low cementation strength is helpful to form a complex fracture network with high conductivity when making a fracturing operation scheme for a conglomerate reservoir, and the conglomerate with high cementation strength is beneficial to extend fractures and form a large-scale fracture network.

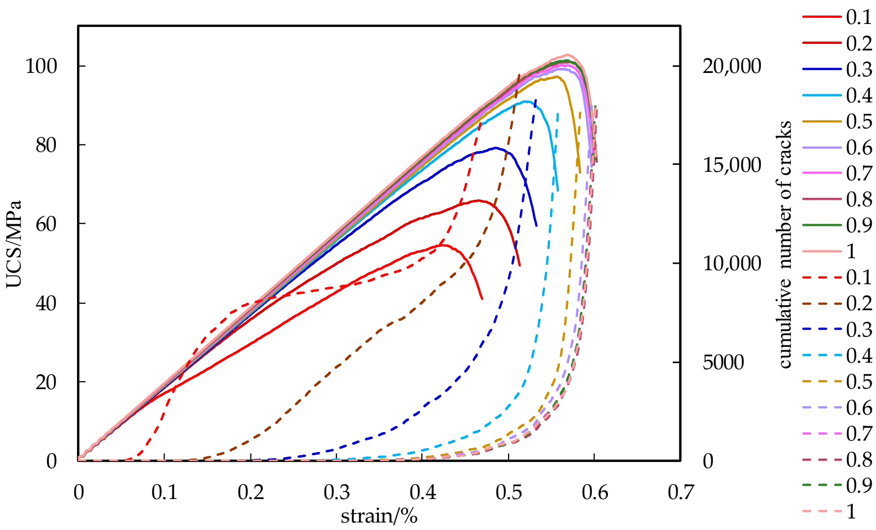

Figure 4. Accumulated cracks and stress–strain curves under different cementation strength ratios.

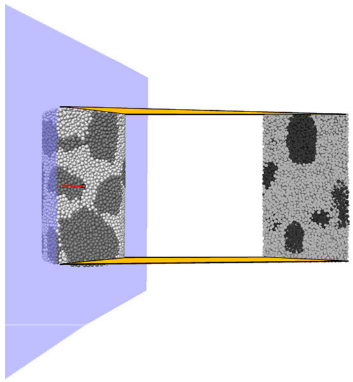

(**a**)

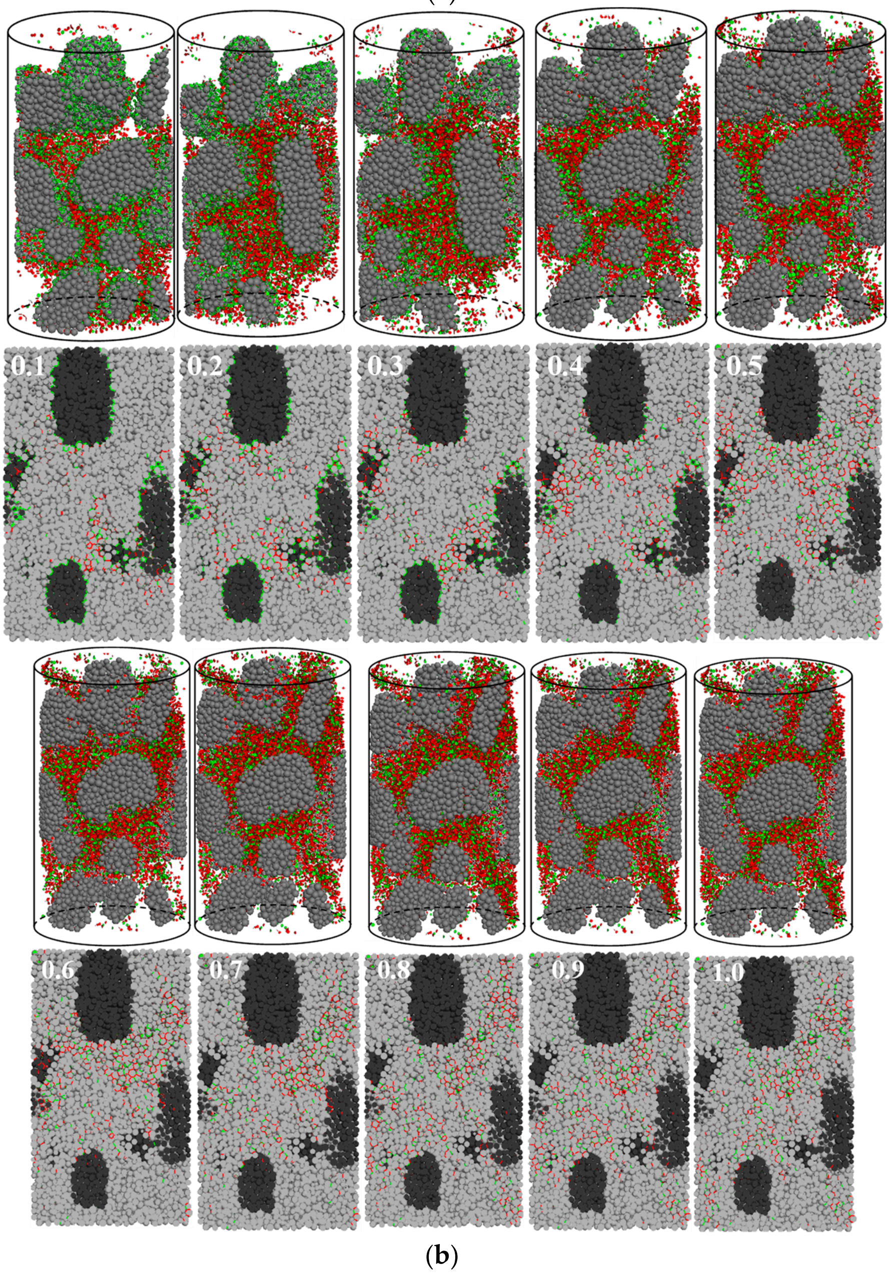

(**b**)

Figure 5. Fracture propagation patterns with different cementation strength. (**a**) Projection diagram of three-dimensional discrete element model; (**b**) Crack morphology under uniaxial compression with different cementation strength ratios (shearing cracks in green and tensile cracks in red).

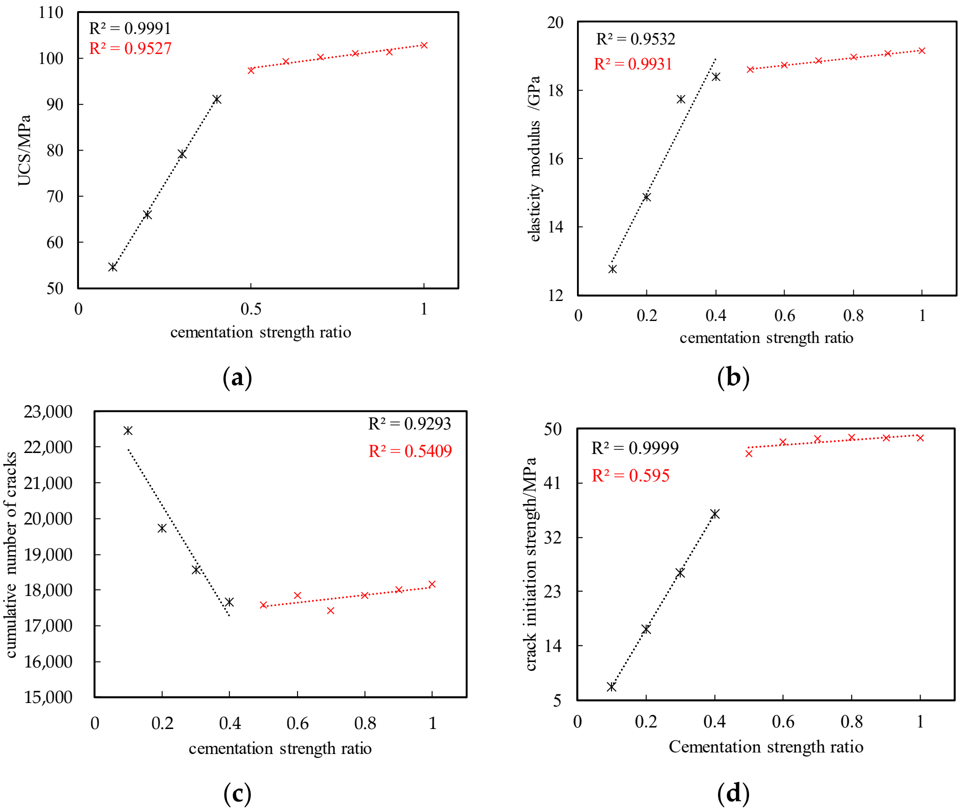

Figure 6. Influence of different cementation strengths on mechanical parameters and cumulative number of cracks. (**a**) Ratio of compressive strength to cementation strength; (**b**) Ratio of elastic modulus to bond strength; (**c**) Ratio of cumulative number of cracks to cementation strength; (**d**) Ratio of crack initiation strength to cementation strength.

3.2. Gravel Content

The complex sedimentary environment and tectonic background of the conglomerate make gravel particles appear in different shapes. According to the practice, the conglomerate models with 20%, 35%, 50%, 60% and 70% gravel content are constructed for the uniaxial compression test. The results show that with the increase in gravel content, the elastic modulus of the conglomerate also increases, and the fracture initiation time of rock is advanced. The reason for this is that with the increase in gravel content, the matrix and cementation area of the conglomerate are destroyed with the continuous compression in the axial direction, while the gravel is displaced without destruction and presents high strength. Due to the high gravel content, with the displacement caused by axial compression, gravels contact each other. The higher the gravel content, the more contact points between gravels [26,27], and the occlusion effect between gravels leads to an increase in the overall strength of gravel. The black scatters in Figure 7a–d show the effect of gravel content on the mechanical properties of the conglomerate. It can be seen that with the increase in gravel content, the elastic modulus and crack initiation strength both increase, and the fitting coefficient is greater than 0.8, which shows that the experiment has practical significance. However, there is no obvious feedback between uniaxial compressive strength, cumulative fracture number and gravel content, which is caused by too few data points and irregular gravel shape. In order to study the relationship between compressive strength and cumulative number of fractures and gravel content, ideal spherical gravel is used for numerical simulation.

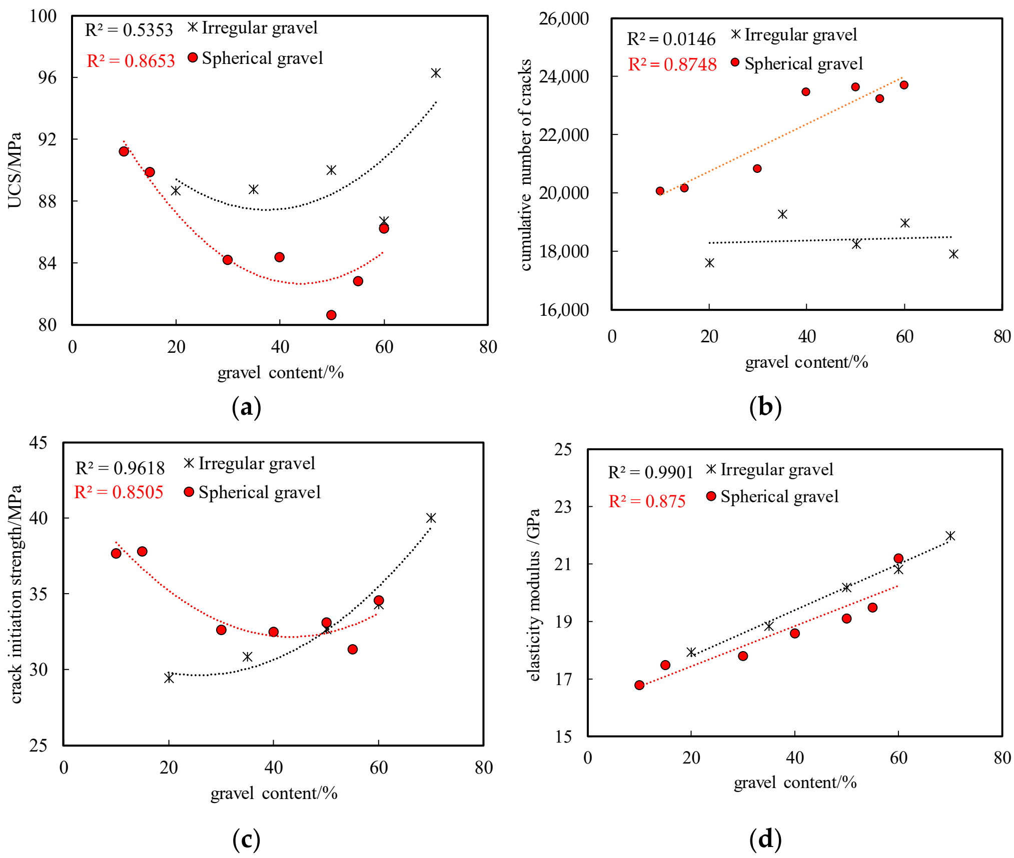

Figure 7. Effects of different gravel content on mechanical parameters and cumulative cracks. (**a**) Reaction between gravel content and ultimate; (**b**) Reaction between gravel content and cumulative; (**c**) Reaction between gravel content and crack initiation strength; (**d**) Reaction between gravel content and elasticity modulus.

Uniaxial compression experiments were carried out on spherical gravel with different contents. As shown in Figure 7, with the increase in spherical gravel content, the elastic modulus of conglomerate increases, while the uniaxial compressive strength decreases when the spherical gravel content is 10~50% and increases when the spherical gravel content is greater than 50%. The reason is that gravel, as a heterogeneous body in the conglomerate, is prone to stress concentration under compression. The closer the distance between two gravels, the greater the additional stress, and the shorter the rock bridge, which is easier to break. Therefore, with the increase in gravel content, the uniaxial compressive strength decreases, and the cumulative number of cracks increases. However, when the gravel content increases to a critical point, the gravel contacts each other in the conglomerate, and the cementation between two contacting gravels is gravel-to-gravel cementation rather than weak gravel-to-matrix cementation, which will lead to an increase in the overall strength of the conglomerate as shown in the red box in Figure 8. In addition, when the conglomerate with high gravel content is compressed, the original non-contact gravel squeezes each other and bears a part of the pressure due to axial compression, which leads to the matrix compression of the conglomerate being converted into gravel compression. As the gravel content increases, the compressive strength of conglomerate increases, and the cumulative number of fractures decreases or tends to be flat.

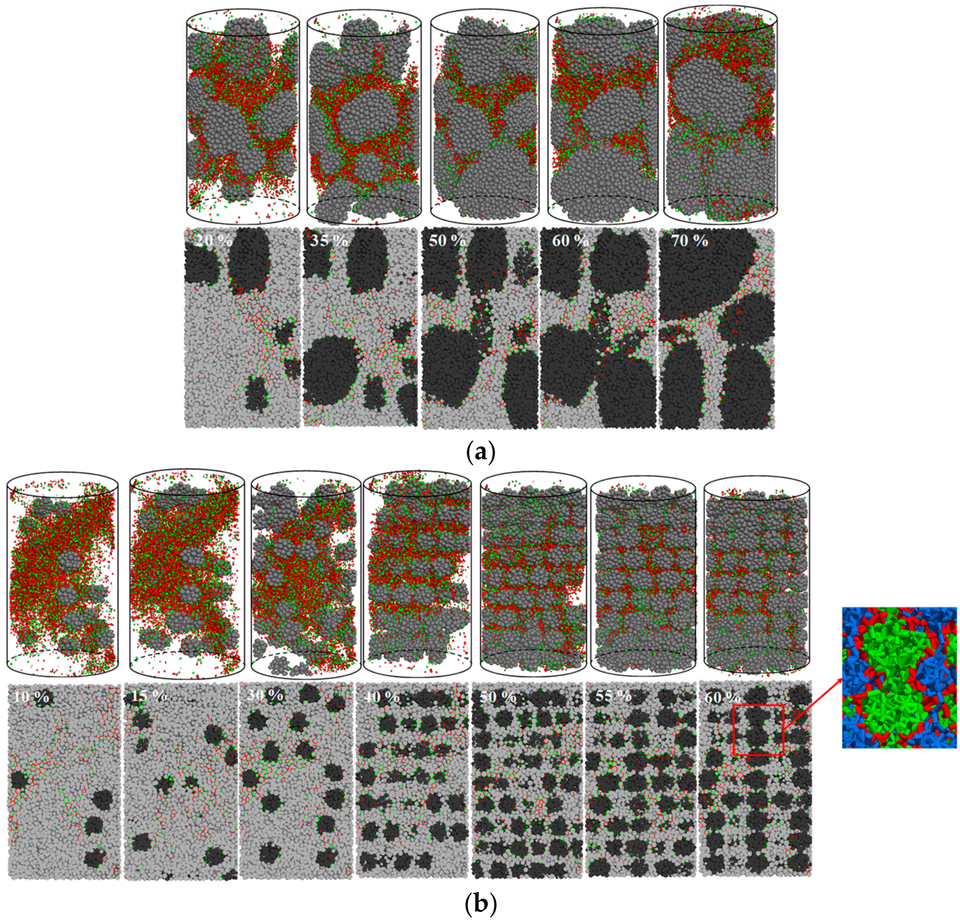

Figure 8. Distribution of cracks with different gravel content. (**a**) Fracture distribution of irregular gravel with different content; (**b**) Fracture distribution of spherical gravel with different content.

Effects of different contents of spherical gravel on crack initiation pressure, compressive strength, cumulative fracture number and elastic modulus, as shown in red circular marks in Figure 7a–d, show that the above four parameters all change regularly with the increase in gravel content. The elastic modulus and spherical gravel content show a positive correlation. The cumulative number of fractures increases first and then tends to be flat with the increase in spherical gravel content. The fracture initiation pressure decreases first and then tends to be flat with the increase in gravel content. When the gravel content is more than 50%, the fracture initiation pressure shows an upward trend.

According to the distribution map of fractures after failure, there are three main propagation forms of fractures in the conglomerate: crack arrest, bypassing gravels and penetrating gravels. When the content of irregular gravel is 20~35%, cracks are mainly produced by shear force, and the cracks will bypass gravel, which is called bypassing gravel. When the content of irregular gravel is more than 50%, bypassing gravel becomes the major force of crack propagation and is accompanied by penetrating gravel. The fracture propagation morphology of the conglomerate with different gravel content after uniaxial compression is observed, and most of the fractures after failure, are caused by tensile force, as shown in Figure 8a. When the content of spherical gravel is 10%, fractures mainly extend in the conglomerate matrix, and there are few phenomena of penetrating gravel or bypassing gravel. When the content of spherical gravel increases, the phenomenon of penetrating gravel and bypassing gravel increases, which leads to more complex fracture morphology and an increase in the number of shear fractures around gravel. When the gravel content is 55%, the cumulative number of fractures reaches the peak, with a most complex fracture network. When the content of spherical gravel is more than 55%, the cumulative number of fractures decreases, and the fracture shape tends to be single, showing oblique intersecting fractures as shown in Figure 8b. Compared with spherical and irregular gravel with different contents, when the gravel content is high, the fracture network after compression is less complex than spherical gravel because the single particle size of irregular gravel is larger and the fracture is not easy to pass through the larger particle size gravel.

In fracturing operation, temporary plugging and other measures can be taken to make fractures produce branch fractures to form a complex fracture network for reservoirs with low gravel content, and cyclic fracturing can be taken to bypass gravel and finally form a complex fracture network with main fractures for conglomerates with high gravel content under low water pressure.

4. Discussion

A conglomerate reservoir shows a strong heterogeneity due to its complex sedimentary environment and tectonic setting, and the mechanical properties of the conglomerate reservoir can only be studied on a macroscopic scale by laboratory mechanical experiments. Different from the traditional indoor test, the numerical simulation based on the discrete element method can easily extract the detailed information of basic particle position, contact force and other parameters [20], and conduct an in-depth analysis.

The interaction between two adjacent particles in a particle aggregate can be described by the normal contact force, the normal contact force perpendicular to the contact plane, and the tangential contact force parallel to the contact surface. Sun [28] put forward a cross-scale correlation for analysis, pointing out that the mechanical parameters of particles determine the force chain and its stability of materials, while the complex dynamic response of the force chain network determines the macroscopic mechanical properties of materials. Therefore, it is of practical significance to study the fabric characteristics of particles to reveal their macroscopic mechanical characteristics based on the basic components of the discrete element.

The geometric anisotropy of conglomerate discrete element particles is usually composed of its particle contact normal and branch vector. In this paper, the fabric tensor is used to quantify the contact force between conglomerate particles.

$$\varnothing_{ij} = \frac{1}{N_c}\sum_{C=1}^{N_c} n_i^c n_j^c \tag{2}$$

In Formula (2), $\varnothing_{ij}$, N_c, n_i^c are the normal fabric tensor, unit vector and total contact number, respectively. The second order anisotropic tensor of normal contact is:

$$\alpha_{ij}^c = \frac{15}{2}\varnothing_{ij}^{'} \tag{3}$$

In Formula (3), $\varnothing_{ij}^{'}$ is the partial tensor of $\varnothing_{ij}$. The mechanical anisotropy mainly depends on the contact force related to the direction of the contact plane. It can be divided into the anisotropy of the normal and tangential contact forces, as shown below:

$$\varnothing_{ij} = \frac{1}{N_c}\sum_{C=1}^{N_c} n_i^c n_j^c \tag{4}$$

$$X_{ij}^n = \frac{1}{N_c}\sum_{C=1}^{N_c} \frac{f^n n_i n_j}{1+\alpha_{kl}^c n_k n_l} \tag{5}$$

$$X_{ij}^t = \frac{1}{N_c}\sum_{C=1}^{N_c} \frac{f^t t_i n_j}{1+\alpha_{kl}^c n_k n_l} \tag{6}$$

$$\alpha_{kl}^{n} = \frac{15}{2}\frac{X_{ij}^{\prime n}}{\overline{f}^{0}} \tag{7}$$

$$\alpha_{kl}^{t} = \frac{15}{3}\frac{X_{ij}^{\prime t}}{\overline{f}^{0}} \tag{8}$$

In Formula (8), X_{ij}^{n} is the normal fabric tensor of particle contact force; X_{ij}^{t} is the tangential fabric tensor of particle contact force, f^{n}, f^{t} are the values of normal and tangential contact force respectively; $\overline{f}^{0}$ and $X_{ij}^{\prime n}$ are the average normal contact force; $X_{ij}^{\prime n}$ and $X_{ij}^{\prime t}$ are the partial tensors of X_{ij}^{n} and X_{ij}^{t}. The anisotropy of particle contact force caused by different factors can be characterized by the above four factors. GUO [29] expressed the degree of anisotropy by the invariant of the partial tensor, as shown in the formula:

$$\alpha^{*} = sign(S_r)\sqrt{\frac{3}{2}\alpha_{ij}^{*}\alpha_{ij}^{*}} \tag{9}$$

In Formula (9), α^{*} is the above four fabric tensors, and the double shrinkage normalized quantities of α_{ij}^{*} and $\alpha_{ij}^{\prime}$ are defined by S_r:

$$S_r = \frac{\alpha_{ij}^{*}\alpha_{ij}^{\prime}}{\sqrt{\alpha_{kl}^{*}\alpha_{kl}^{*}}\sqrt{\alpha_{mm}^{*}\alpha_{mm}^{*}}} \tag{10}$$

In Formula (10), $sign(S_r)$ represents the relative direction of the main direction of α_{ij}^{*} to the stress tensor; A positive α_{ij}^{*} indicates that the principal direction is close to the principal direction of the stress tensor, and a negative sign is the opposite. The discrete element model is meshed to ensure that the area of each statistical region is equal, and the model is divided into 256 triangular cylinders according to the equal surface area. The height and color of each cylinder changes with the change of statistical strength. The higher the height and the darker the color of the cylinder, the more concentrated the distribution is. The closer the shape of fabric tensor is to the sphere, the smaller its anisotropy coefficient is.

Figure 9 shows the normal contact force distribution of the conglomerate rock sample with the calibration parameters at different loading stages. It can be seen from the figure that the distribution shape of the particle contact system in the initial state is approximately a sphere, as shown in point A in Figure 9. The normal contact force in the particle system of the rock sample is uniform, and the anisotropy coefficient is close to zero. As the sample is continuously loaded axially to reach the peak strength, as shown in point B in Figure 9, the normal contact force of the conglomerate particle system is stretched in the loading direction, that is, the contact normal force increases in the loading direction, and the anisotropy coefficient of the conglomerate increases. The contact force of the particle system method in the post peak stage of continuous loading is further stretched and tends to be stable, and inclines to the right to a certain extent, as shown in point C in Figure 9. This is because the shear cracks around the gravel are generated due to the destruction of the gravel and matrix cementation surface during the loading process, which leads to the complete loss of bearing capacity of the left gravel detached from the conglomerate parent body. The instability failure of the conglomerate is shown in Figure 3a. The anisotropy coefficient of the conglomerate in this stage is the largest in three states. It can be seen that the anisotropy coefficient of the conglomerate increases roughly with the loading process.

Figure 10 shows the distribution of normal contact force after uniaxial compression with different cementing strengths. Zhao [30] thinks that the influence of normal contact force on stress is far greater than that of tangential contact force. Therefore, the distribution and size of normal contact force of the conglomerate under different cementation strengths are emphatically concerned. It can be seen from Figure 10 that when the cementation strength ratio is 0.1, the overall color of the normal contact force distribution of the conglomerate shows a cool color and the shape is similar to a cylinder, which indicates that the normal contact force of the conglomerate is small, the anisotropy coefficient is large and the heterogeneity of the conglomerate is strong. With the increase in the cementation strength ratio, the color of normal contact force distribution of the conglomerate gradually changes from a cool color to a warm color, and the color of the axial end cylinder gradually changes from green to red, which indicates that the overall strength of the conglomerate increases with the increase in normal contact force, which is consistent with the trend that uniaxial compressive strength increases with the increase in the cementation strength ratio. With the increase in the cementation strength ratio, the distribution of normal contact force gradually tends from a cylinder to a sphere, which indicates that the anisotropy coefficient of the conglomerate gradually decreases with the increase in the cementation strength ratio, and the heterogeneity of the conglomerate decreases.

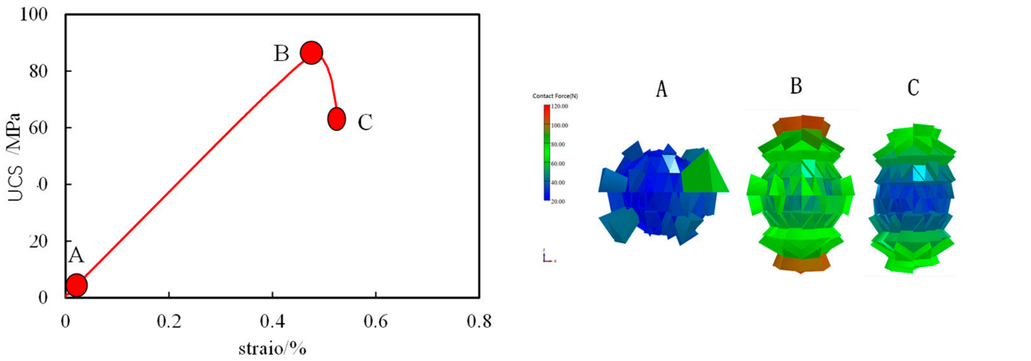

Figure 9. Normal contact force distribution in different states.

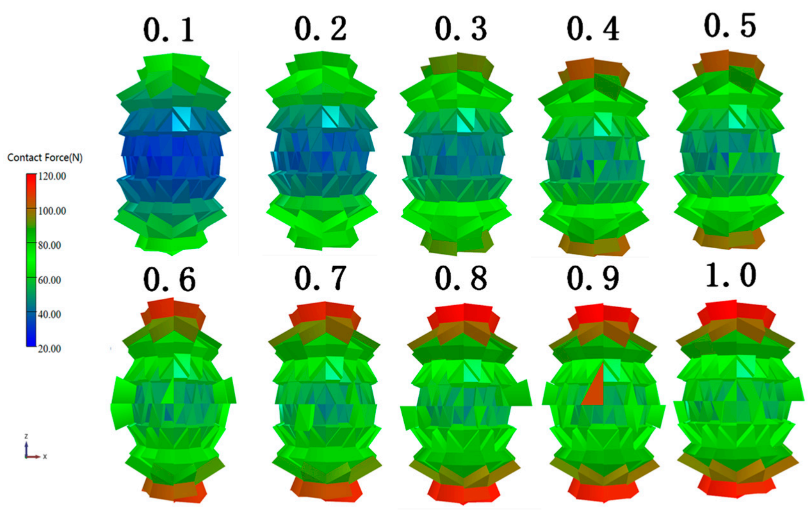

Figure 10. Normal contact force distribution of different cementation strength ratios.

From the data of normal contact force, it can be seen that when the cementation strength of the conglomerate is low, additional stress is more likely to occur on the cementation surface between gravel and matrix under a compression condition, which leads to the sliding between gravel and matrix and the formation of shear cracks around gravel on the cementation surface. These fractures and stresses cause the conglomerate with low cementation strength to be damaged locally and produce fractures, which makes the overall strength of the conglomerate low. With the increase in cementation strength, the overall fabric of the conglomerate in the compression state is more uniform, the stress concentration phenomenon is weakened and fractures are not easy to bypass gravel, which makes the overall strength of the conglomerate increase, the fracture initiation pressure increase and the cumulative number of fractures decrease. When the cementation strength ratio is less than 0.4, the mechanical properties and fracture propagation of the conglomerate are mainly affected by cementation strength. When the cementation strength ratio is greater than 0.4, gravel content and shape play a leading role in fracture propagation. When fracturing the conglomerate reservoir, the actual construction plan should consider the two factors of cementation strength and gravel content. The conglomerate reservoir with low cementation strength and high gravel content is conducive to the formation of a complex fracture network with a certain scale and high conductivity by bypassing or penetrating the gravel.

5. Conclusions

In this paper, a three-dimensional numerical model of gravel is established by the discrete element method to study the influence of cementation strength and gravel content on mechanical properties and the crack propagation law of the conglomerate, and the simulation results are analyzed by micromechanics. The main conclusions are as follows:

(1) With the increase in the cementation strength ratio, the uniaxial compressive strength and elastic modulus of the conglomerate increase, the number of accumulated fractures decreases, and the conglomerate changes from plasticity to brittleness. When the cementation strength ratio is greater than 0.4, the mechanical parameters of the conglomerate do not change significantly.
(2) The elastic modulus of the conglomerate increases with the increase in gravel content. When the gravel content increases from 10% to 50%, the uniaxial compressive strength of the conglomerate decreases, and the fracture network is simple after failure. When the gravel content is more than 50%, the uniaxial compressive strength of the conglomerate increases, the cracks propagation phenomenon is mainly bypassing gravel accompanied by penetrating gravel, and the fracture network is more complex. When fracturing the conglomerate reservoir with low gravel content to increase production, measures such as temporary plugging should be taken to make fractures produce branch fractures to form a complex fracture network.
(3) The lower the cementation strength, the lower the normal contact force, the higher the anisotropy coefficient and the stronger the heterogeneity of the conglomerate. Different cementation strengths of the conglomerate show different mechanical properties, which is caused by different transmission and evolution laws of contact force between internal particles, and their mechanical properties are external macroscopic manifestations of contact force between internal particles.

Author Contributions: Conceptualization, J.Z., X.L. and W.Z.; methodology, J.X.; validation, L.L., X.L. and J.X.; investigation, J.Z.; data curation, J.Z.; writing—original draft preparation, W.Z.; writing—review and editing, W.Z.; visualization, J.Z.; project administration, L.L.; funding acquisition, L.L. All authors have read and agreed to the published version of the manuscript.

Funding: This research is supported by the Young Scientific and Technological Innovation Team of Rock Physics in Unconventional Strata of Southwest Petroleum University (No. 2018CXTD13).

Institutional Review Board Statement: Not applicable.

Informed Consent Statement: Not applicable.

Data Availability Statement: Not applicable.

Conflicts of Interest: The authors declare no conflict of interest.

References

1. Zhao, Z.; Du, H. *Exploration and Development of Unconventional Oil and Gas Resources: Tight Oil and Gas*; Petroleum Industry Press: Beijing, China, 2012.
2. He, Y.C.; Zhang, C.R. The world's largest conglomerate oil field discovered in Junggar Basin, Xinjiang. *Geol. China* **2017**, *44*, 1174.

3. Ding, X.; Zhang, L.; Zhu, H. Effect of Model Scale and Particle Size Distribution on PFC3D Simulation Results. *Rock Mech. Rock Eng.* **2014**, *47*, 2139–2156. [CrossRef]
4. Xiao, P.; Zhang, L. Loading rate effects on cracking behavior of flaw-contained specimens under uniaxial compression. *Int. J. Fract.* **2013**, *180*, 93–110.
5. Chen, C. Engineering geological characteristics of conglomerate in Xiyu formation, Xinjiang. *China Water Transp.* **2013**, *13*, 244–246.
6. Chen, C.; Wang, J.; Yu, T.; Li, Y.; Zou, S.; Liu, L. Migration law of fracture proppant in conglomerate reservoir of Wuerhe formation in Mahu depression. *Xinjiang Pet. Geol.* **2021**, *42*, 559–564.
7. Ju, Y.; Yang, Y.; Chen, J.; Liu, P.; Dai, T.; Guo, Y. Three dimensional reconstruction and hydraulic fracturing simulation of low permeability heterogeneous sandy conglomerate. *Sci. Bull.* **2016**, *61*, 82–93.
8. Liu, G.; Cai, M.; Huang, M. Mechanical properties of brittle rock governed by micro-geometric heterogeneity. *Comput. Geotech.* **2018**, *104*, 358–372. [CrossRef]
9. Khanlari, G.; Heidari, M.; Noori, M.; Momeni, A. The effect of petrographic characteristics on engineering properties of conglomerates from Famenin Region, Northeast of Hamedan, Iran. *Rock Mech. Rock Eng.* **2016**, *49*, 2609–2621. [CrossRef]
10. Ma, D.; Luo, Y.; Hu, D. Study on the influence mechanism of particle size sorting and confining pressure on hydraulic fracturing fracture of sandy conglomerate. *Res. J. Rock Mech. Eng.* **2020**, *39*, 2264–2273.
11. Tang, P. Experimental study on brittle characteristics of sandy conglomerate reservoir in Songbei tight gas reservoir. *Oil Gas Geol. Recovery* **2019**, *26*, 46–52.
12. Liu, X.; Xiong, J.; Liang, L.; You, X. Rock mechanical characteristics and fracture propagation mechanism of glutenite reservoir of Baikouquan formation in Mahu depression. *Xinjiang Pet. Geol.* **2018**, *39*, 83–91.
13. Afifipour, M.; Moarefvand, P. Mechanical behavior of bimrocks having high rock block proportion. *Int. J. Rock Mech. Min. Sci.* **2014**, *65*, 40–48. [CrossRef]
14. Ding, X.; Zhang, H.; Huang, S.; Lu, B.; Zhang, Q. Study on mechanical properties of unsaturated soil rock mixture based on meso numerical test. *J. Rock Mech. Eng.* **2012**, *31*, 1553–1566.
15. Li, L.; Li, G.; Meng, Q.; Wang, H.; Wang, Z. Numerical simulation of propagation of hydraulic fractures in glutenite formation. *Rock Soil Mech.* **2013**, *34*, 1501–1507.
16. Jin, C. *Study on Mechanical Properties and Fracture Law of Conglomerate Reservoir*; China University of Petroleum: Beijing, China, 2017.
17. Cundall, P. Computer Interactive Graphics and the Distinct Element Method. In *Rock Engineering for Foundations & Slopes*; American Society of Civil Engineers: Reston, VA, USA, 2010.
18. Luo, P.; Li, Y.; Jiang, Y.; Li, Y. Simulation of hydraulic fracture propagation path in sandy gravel. *Oil Gas Geol. Recovery* **2013**, *20*, 103–106.
19. Han, Z.; Zhang, L.; Zhou, J.; Ni, Y. Study on heterogeneous effect of mineral particle size based on PFC2D simulation. *J. Eng. Geol.* **2019**, *27*, 706–716.
20. Lei, X.; Yang, Z.; Zhai, H.; Hu, Y. Particle flow numerical study on Influencing Factors of block stone crushing of earth rock mixture. *J. Eng. Geol.* **2020**, *28*, 1193–1204.
21. Jiang, M.; Zhang, N.; Shen, Z.; Chen, H. Discrete element analysis of crackpropagation mechanism in uniaxial compression of fractured rockmass. *Geotech. Mech.* **2015**, *36*, 3293–3300.
22. Deng, S.; Zheng, Y.; Feng, P. Application of experimental design method in meso parameter calibration of hard rock PFC ~ (3D) model. *J. Geotech. Eng.* **2019**, *41*, 655–664.
23. Yang, B.; Jiao, Y.; Lei, S. A study on the effects of microparameters on macroproperties for specimens created by bonded particles. *Eng. Comput.* **2006**, *23*, 607–631. [CrossRef]
24. Cundall, P.; Strack, O. A discrete numerical model for granular assemblies. *Geotechnique* **1979**, *29*, 47–65. [CrossRef]
25. Zhang, B.; Zhang, C.; Wang, C.; Hao, B. Calibration Method of Meso-Parameters of PFC^{2D} Flat-Joint Model. *J. Comput. Mech.* **2021**, *38*, 665–673.
26. Wang, X.; Wang, X.; Shen, J.; Zhu, C. Particle size and confining-pressure effects of shear characteristics of coral sand: An experimental study. *Bull. Eng. Geol. Environ.* **2022**, *81*, 97. [CrossRef]
27. Wang, X.; Cui, J.; Shen, J.; Wang, X.; Zhu, C. Particle breakage behavior of a foundation filling material on island-reefs in the South China Sea under impact loading. *Bull. Eng. Geol. Environ.* **2021**, *306*, 124690. [CrossRef]
28. Sun, Q.; Song, S.; Jiang, Y.; Jin, F.; Zhang, C. Triaxial mechanical analysis based on particle hydrodynamics. *J. Mech.* **2012**, *44*, 447–450.
29. Guo, N.; Zhao, J. The signature of shear-induced anisotropy in granular media. *Comput. Geotech.* **2013**, *47*, 1–15. [CrossRef]
30. Zhao, S. *Discrete Element Investigation of Physical and Mechanical Properties of Granular Materials*; South China University of Technology: Guangzhou, China, 2018.